Progress In Electromagnetics Research Letters, Vol. 104, 77–85, 2022

U-Slotted Elliptical Shape Patch Antenna for UWB On-Body Communications

Pasumarthi Amala Vijaya Sri and Ketavath Kumar Naik*

Abstract—An elliptical shape patch (ESP) antenna with inverted U-shaped slots is proposed and presented in this paper for on-body communications. A coplanar waveguide (CPW) feed is used as ground to produce impedance matching, and inverted U-shaped slots are used to produce the ultra-wideband (UWB). The proposed ESP antenna model covers UWB characteristics in free space, and it is observed at 3 to 10.7 GHz. When it is implanted on a flat tissue model of human body, the bandwidth is 2.2 to 10.8 GHz. The SAR values of 1.26 W/kg and 1.58 W/kg are observed on-body at 4.9 GHz and 7.3 GHz operating frequencies, respectively. The results with respect to the radiation pattern, gain, reflection coefficient, and surface current distribution are also presented.

1. INTRODUCTION

In recent years, extensive research work has been carried out in biomedical applications using microstrip antennas for health monitoring systems. As these antennas are used in implantable medical devices (IMDs), they should be light in weight, bio-compatible, and conform to the human body. Although various biomedical frequency bands already exist, microstrip patch antennas have peculiar characteristics, so it also covers ultra-wideband (UWB) and is used for on-body centric wireless communications.

Implantable medical devices with wireless networks can be implanted anywhere on the human body, at least conceptually. As the battery life of these IMDs is limited, they need to be recharged frequently. This problem can be solved by using wearable repeaters [1], which enhance the link between the IMDs and the patients without any wire connections to the battery. There are some limitations imposed by the antennas operating in the MICS and ISM bands when they are employed for on-body applications. In real time situation, MICS band antennas provide low bandwidth, require high data rate and large dimensions. The ISM band antenna provides low data rate transmission. These limitations in MICS and ISM band antennas can be overcome by designing the antennas for UWB frequency.

In the literature, various antenna models are designed for UWB applications [2, 3], such as the elliptical shape monopole antenna [4], tapered slot antenna [5], reconfigurable antenna [6], and circular patch antenna [7] with elliptical slot on ground plane, were designed for UWB application. In [4], a half modified circular shape ground plane was considered, and a radiating efficiency of more than 90% was obtained. Similarly, in [5] rectangular slits at the edges were designed to produce wide bandwidth of 8.45 GHz. A maximum gain of 7.55 dBi was obtained for this antenna. In [8], a notch was considered to achieve the impedance matching between patch and ground plane to operate the antenna for UWB.

The experimental campaign of medical body area network (BAN) in hospital environment was studied in [9], using flexible antenna models for various frequency bands. In [10], a dual-band filtering microstrip antenna was designed for UWB application from 2.35 to 12.796 GHz. A band rejection from

Received 30 January 2022, Accepted 10 May 2022, Scheduled 26 May 2022
* Corresponding author: Ketavath Kumar Naik (kumarvtr@gmail.com).
The authors are with the Antenna Research Laboratory, Department of Electronics and Communication Engineering, Koneru Lakshmaiah Education Foundation (KLEF), K L University, Vaddeswaram, Guntur, AP, India.

4.9 to 5.98 GHz and 7.15 to 7.99 GHz was observed, and this antenna model was used for bio-medical imaging systems and medical telemetry applications. A rectangular adhesive bandage like antenna model in [11] was designed with 89.5% bandwidth in free space and 44.7% when being placed on the tissue equivalent phantom. This antenna model has been used for wireless telemetry services. In [12], three antenna models were designed for UWB applications, and the proposed antenna model analysis was carried out by varying the distance from the antenna to the human body. A planar inverted cone antenna model [13], with a double layer substrate for UWB application, was designed, and an impedance bandwidth in the ratio of 13 : 1 was obtained. A Koch fractal slot antenna [14], for UWB application, operated for 2.85 to 12 GHz frequency with notch band characteristics from 4.65 to 6.40 GHz. This frequency notched function and size reduction were achieved by using a Koch fractal slot. A tapered patch antenna was designed in [15], to evaluate the performance of the antenna with the change in the limb movements of the human hand for health care monitoring. This antenna model analysis was carried out at 3, 6, 9 GHz, and the changes in the radiation performance were studied. In [16], an X-slot patch antenna was presented for wider impedance band. In [17, 18], a planar inverted cone antenna and flexible rectangular patch antenna were designed with coplanar waveguide (CPW)-feed. The analysis of antenna in [17] was carried out for on-body application and used for wearable applications. A conformal patch antenna with parasitic elements [19] and split ring resonators [20] was presented for biomedical applications.

In this paper, an elliptical shape patch (ESP) antenna is designed with inverted U-shaped slots for the operation in UWB frequency range, specifically, from 3 to 10.7 GHz. The proposed ESP antenna is implanted in the free-space on a flat three-layer tissue that emulates the human body. The ESP antenna resonates in 3 to 10.7 GHz frequency range, with impedance bandwidth of about 7.7 GHz.

2. ELLIPTICAL SHAPE PATCH ANTENNA DESIGN

The proposed antenna prototype is designed with an elliptically shaped patch and CPW feed as depicted in Fig. 1(a). The elliptical shape patch antenna is fabricated on an FR-4 substrate with a dielectric constant of 4.4 and a loss tangent of 0.01. The length l_1 and width w_1 are the dimensions of the substrate material with a height of 1.6 mm. The elliptical shape patch antenna is deposited on the dielectric substrate, with major and minor radii of r_1 and r_2, respectively. An impedance of 50 Ω is given as input to the ESP antenna through a rectangular stub length of l_2 and a width of w_2. Two inverted U-shape slots are etched from the radiating patch as shown in Fig. 1(a). The dimensions of the two U-shaped slots are l_4, l_5, w_4, w_5, s_1, s_2, s_3, and s_4, respectively. Two rectangular shape radiating patches, with a length of l_3 and width of w_3, are coated on both sides of the feed line, which works as

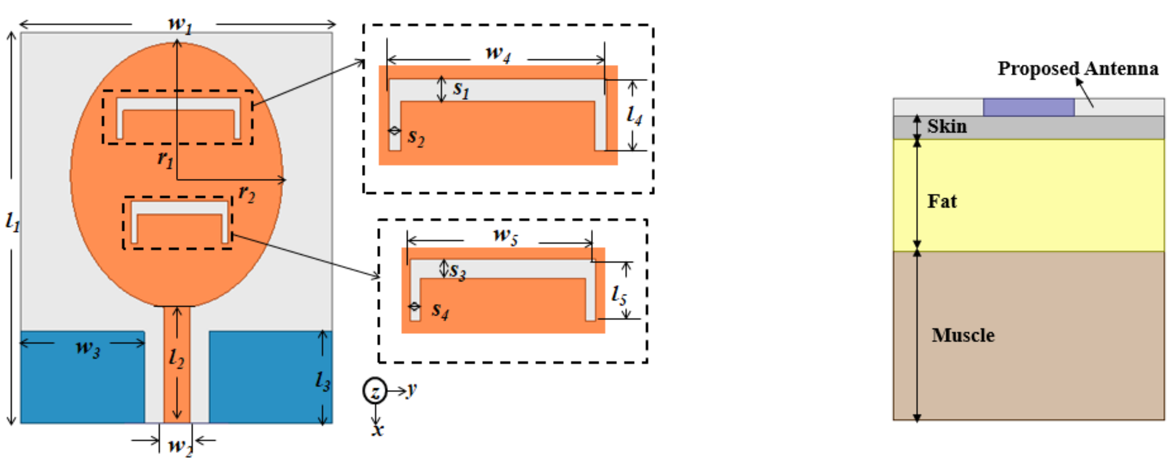

(a) (b)

Figure 1. Geometry of the proposed model (a) elliptical shape patch antenna, (b) flat human body tissue model.

Table 1. Dimensions of the proposed ESP antenna model.

Parameter	Value (mm)	Parameter	Value (mm)
l_1	30	l_5	3.2
w_1	24	w_5	7.5
l_2	9	r_1	10.2
w_2	2	r_2	8
l_3	7	s_1	1
w_3	9.5	s_2	0.5
l_4	3.2	s_3	1
w_4	9.5	s_4	0.5

ground plane with CPW-feed. The dimensions of the proposed antenna model are listed in Table 1.

The proposed antenna prototype is tested in two distinct operating conditions; the free-standing mode and when being attached to a human-body. The on-body measurement is performed by considering the flat human body tissue model with a three-layer structure as shown in Fig. 1(b). The ESP antenna is placed on the skin layer. The height of the skin is considered as 2 mm, fat as the second layer with height of 10 mm, and muscle tissue as the third layer with height of 15 mm, respectively. The dielectric properties of the aforementioned tissue layers in the frequency range from 1 to 15 GHz are listed in Table 2.

Table 2. Typical dielectric properties of human tissues in the 1–15 GHz frequency range.

Tissues	Dielectric constant (ε_r)	Loss tangent (δ)	Thickness
Skin	40–26.2	0.347–0.636	2 mm
Fat	5.42–4.25	0.158–0.264	10 mm
Muscle	54.3–36.1	0.28–0.596	15 mm

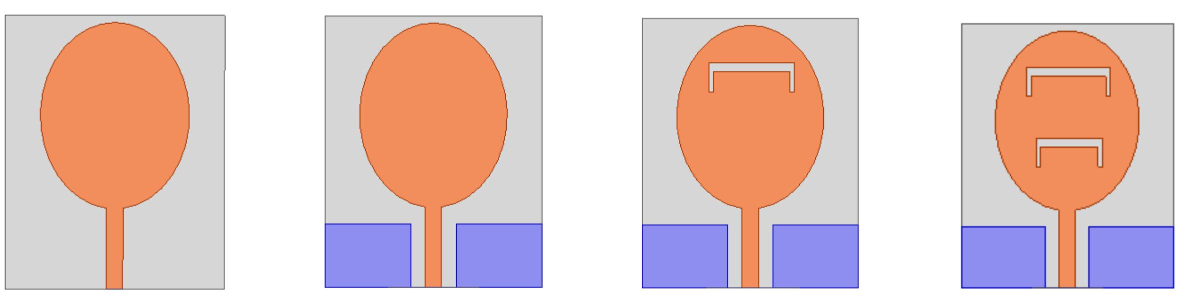

(▯) (c) (▯) (▯)

Figure 2. Evaluation process of the proposed antenna (a) Ant-1, (b) Ant-2, (c) Ant-3, and (d) Ant-4.

The evaluation process of the proposed antenna model is shown in Fig. 2. In the first step, a basic elliptical shape patch antenna (Ant-1) with full ground is considered as shown in Fig. 2(a) for this model, and the antenna resonates for a single band and with low reflection coefficient. To improve the bandwidth as well as achieve the impedance matching, CPW feed (Ant-2) is considered as the ground plane as shown in Fig. 2(b). As can be seen in this figure, Ant-2 resonates from 7.82 to 10.7 GHz frequency band. To operate the antenna in the UWB frequency band, an inverted U-shaped slot is etched from the elliptical patch, resulting in Ant-3 as shown in Fig. 2(c), and the antenna resonates from 6.8 to 10.7 GHz frequency. The second inverted U-shape slot is etched from the patch as shown

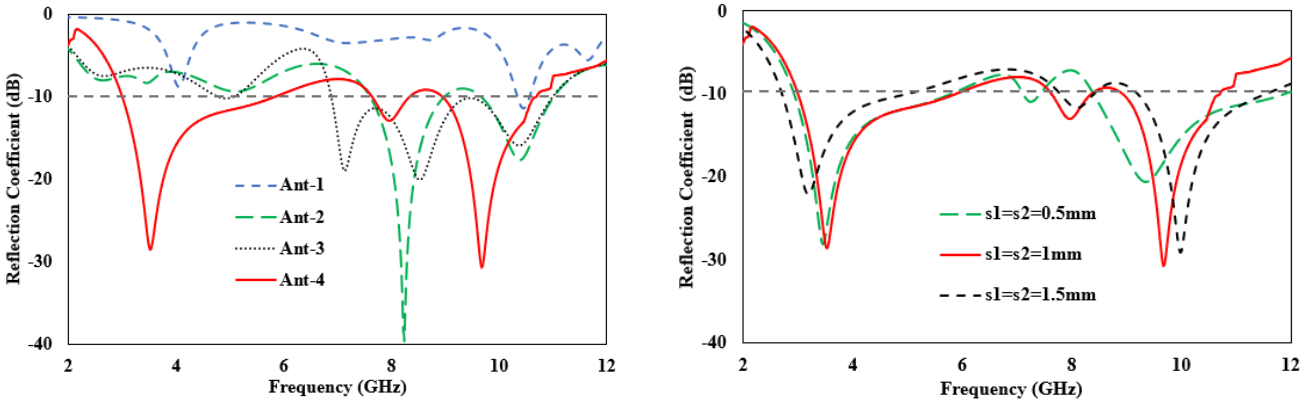

(a) (b)

Figure 3. Reflection coefficient plot for (a) evaluation process, (b) varying $s1$ and $s2$.

in Fig. 2(d), and the antenna operates from 3 to 10.7 GHz frequency band. The corresponding plot for the reflection plot of the proposed antenna evaluation process is shown in Fig. 3(a).

The parametric analysis of the ESP antenna is carried out by varying the slot width ($s1$ and $s2$) of inverted U-shaped slot by 0.5 mm, 1 mm, and 1.5 mm, respectively. The performance of ESP antenna with respect to reflection coefficient is shown in Fig. 3(b). The slot width of 1 mm shows better result both with respect to frequency band and return loss.

3. RESULTS AND DISCUSSION

The analysis of the proposed ESP antenna with respect to free space and on the three-layer tissue model is carried out in EM simulation software. The fabrication of the proposed antenna is shown in Fig. 4(b). Similarly, the measurement setup for the proposed antenna in free space and on-body measurement is shown in Figs. 4(a) and 4(c). Fig. 5 shows the reflection coefficient plot of simulated and measured antenna in free space and on the three-layered model. From Fig. 5, the simulated and measured antennas resonate for UWB 3 to 10.7 GHz, respectively. The operating frequencies and reflection coefficient for the antenna placed in free space and on three layered structure are tabulated in Table 3.

If the air gap (d) is considered between prototype antenna and hand of the human body at different conditions, i.e., $d = 0$ mm, $d = 1$ mm, and $d = 3$ mm, the reflection coefficient plot is shown in Fig. 6. A small deviation in the reflection coefficient plot is observed for $d = 1$ mm and $d = 3$ mm. However,

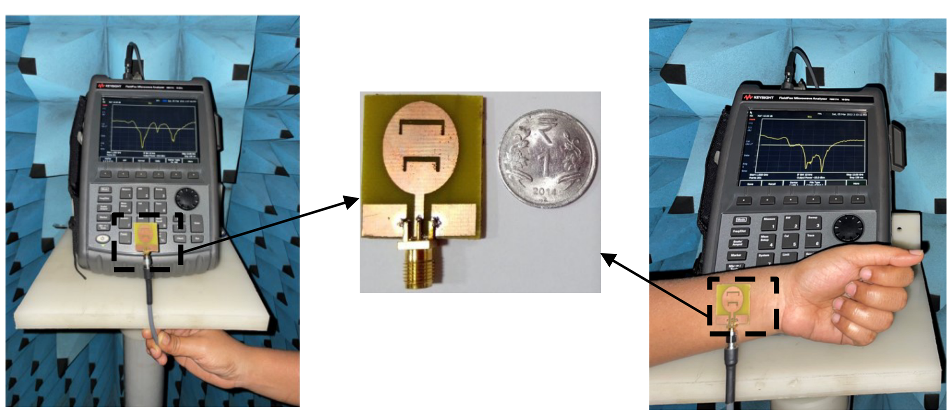

(a) (b) (c)

Figure 4. The proposed ESP antenna (a) free-standing, (b) prototype, and (c) on-body

Table 3. Simulated and measured results of the ESP antenna.

	Free Space		On-Body	
	Operating Frequency (GHz)	Reflection Coefficient (dB)	Operating Frequency (GHz)	Reflection Coefficient (dB)
Simulated	3.52, 7.94, 9.68	−28.59, −13.02, −30.7	4.9, 7.3	−33.2, −28.37
Measured	3.53, 7.88, 9.5	−29.9, −13.48, −32.76	4.58, 7.23	−32.96, −30.46

the proposed prototype antenna works at UWB applications.

The 3D gain plots for the antenna in free space and on the three-layered model are shown in Fig. 7 and Fig. 8. From Fig. 7, the gain values of −2.45 dB, −2.68 dB, and −1.98 dB, are observed at 3.52 GHz, 7.94 GHz, and 9.68 GHz frequencies. Similarly, from Fig. 8, the gain values of −3.6 dB and −2.65 dB are observed at 4.9 GHz and 7.3 GHz frequencies, respectively.

The proposed ESP antenna model analysis is carried out for on body UWB application, and the safety consideration of human body should be considered. The SAR value is restricted for 1 g of tissue to be less than 1.6 W/kg, [13] by IEEE. C95.1-1999. Fig. 9 shows the SAR plots for the antenna implanted on a three layered tissue model. From the plot, the SAR values of 1.26 W/kg and 1.58 W/kg are observed for 4.9 GHz and 7.3 GHz frequencies, respectively.

The co-polarization (Co-Polar) and cross-polarization (Cross-Polar) of ESP antenna with respect to E-plane and H-plane in free space and on a three layered structure are shown in Fig. 10 and Fig. 11. In Fig. 10, the E-plane and H-plane radiation patterns are presented for three frequencies

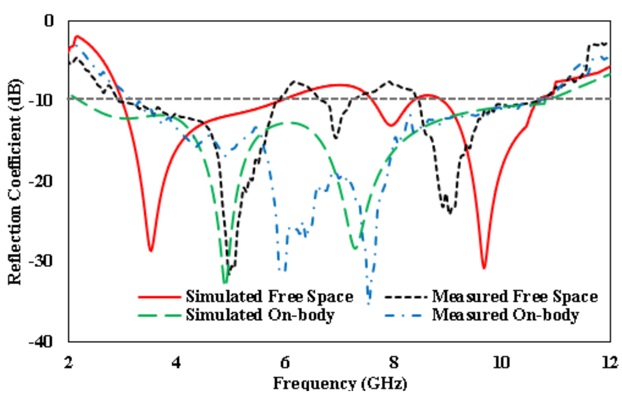

Figure 5. Reflection coefficient of the proposed ESP antenna.

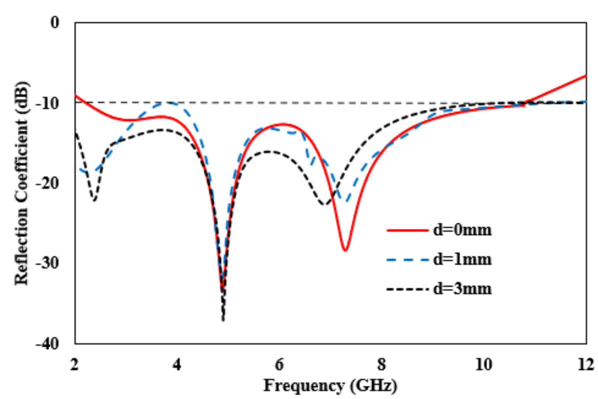

Figure 6. Reflection coefficient plot for air gap between prototype antenna and hand of the human body.

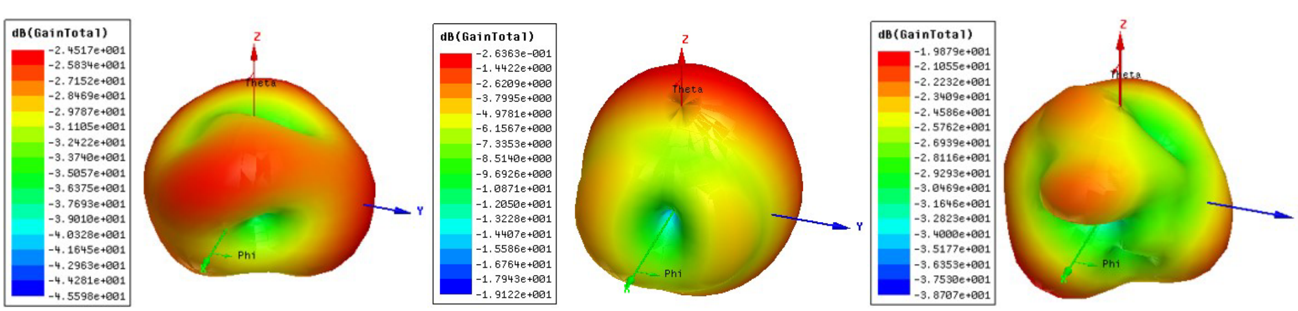

(a) (b) (c)

Figure 7. The 3D gain plot in free space (a) 3.52 GHz, (b) 7.94 GHz, and (c) 9.68 GHz.

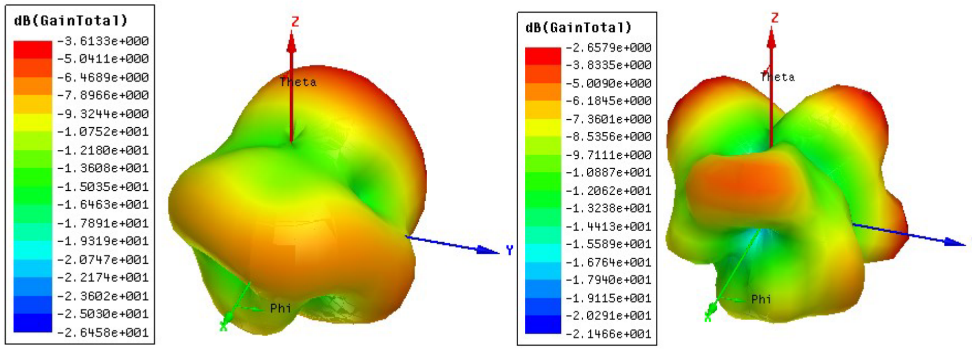

(a) (b)

Figure 8. The 3D gain plot at three-layer tissue model (a) 4.9 GHz, and (b) 7.3 GHz.

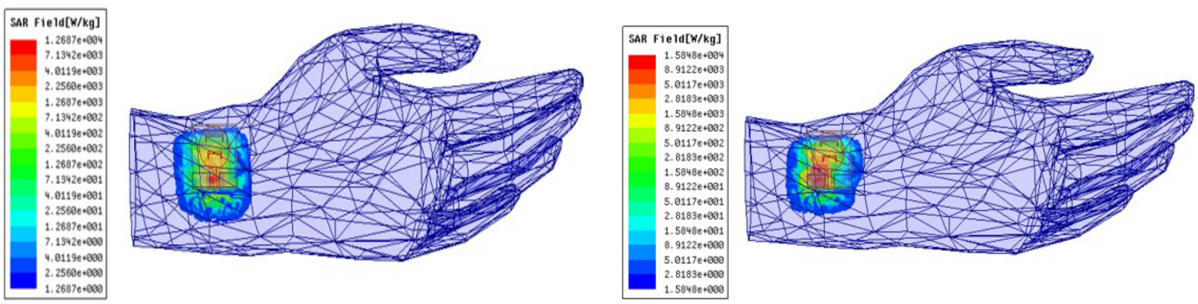

(a) (b)

Figure 9. The SAR of the proposed ESP antenna at frequency (a) 4.9 GHz and (b) 7.3 GHz.

Table 4. Comparison of proposed ESP antenna model with existing model.

Ref.	Antenna Size (mm^2)	Material	Frequency (GHz)	Frequency band	Application
[1]	48.7×40.9	Rubber $\varepsilon_r = 1.485$	2.45	ISM	In-body Wireless Impact
[3]	47.5×50 50×60 100×100	Rt-Duroid $\varepsilon_r = 3$	3 to 6 3 to 6 3 to 9	UWB	On-body application
[4]	30×35	FR-4 $\varepsilon_r = 4.7$	3.1 to 12	UWB	UWB
[6]	20×20	NA	3 to 13.6	UWB	Wi-MAX, WLAN
[8]	41.95×21.2	Rogers 5880	3 to 10.75	UWB	UWB
[18]	31×34	Polyimide	2.5, 5.2	ISM	Wearable telecommunication devices
[19]	25×20	Polyimide	2.45 to 2.48	ISM	ISM Band
[Proposed]	30×24	FR-4	3 to 10.7	UWB	On-body application

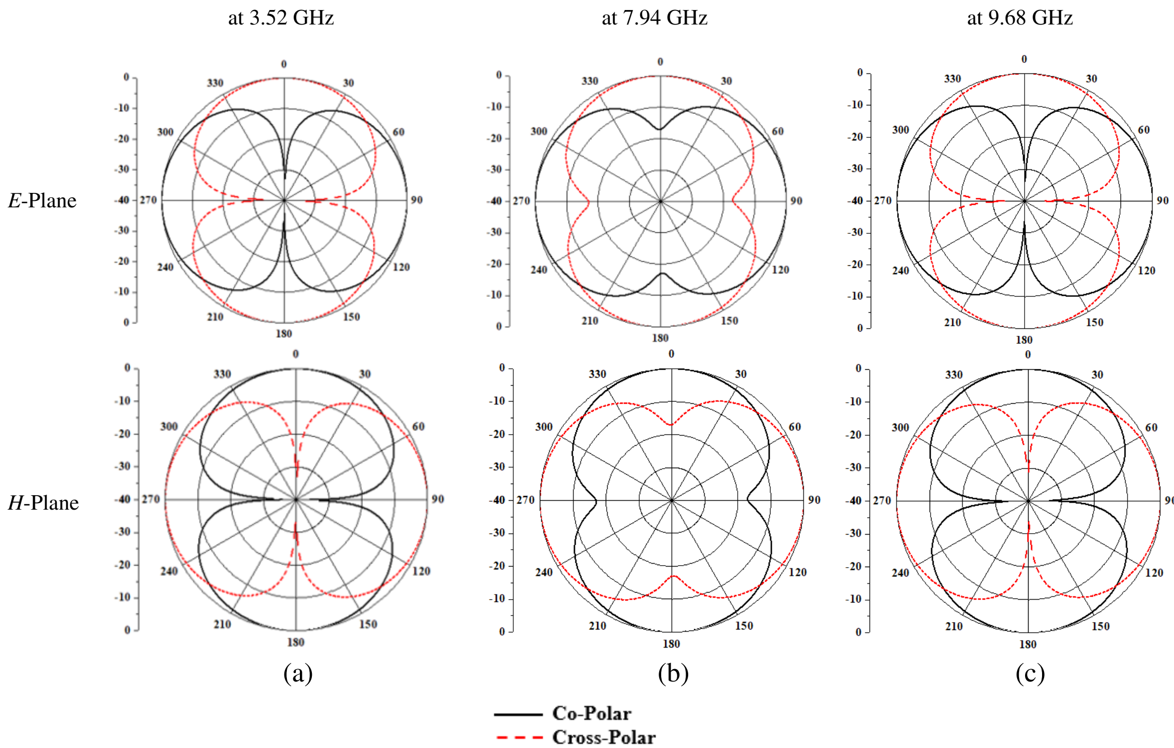

Figure 10. Radiation patterns of ESP antenna in free space at frequencies (a) 3.52 GHz, (b) 7.94 GHz, and (c) 9.68 GHz.

Figure 11. Radiation patterns of ESP antenna on three layered tissue model at frequencies (a) 4.9 GHz, and (b) 7.3 GHz.

at 3.52 GHz, 7.94 GHz, and 9.68 GHz, respectively. Similarly, from Fig. 11, the E-plane and H-plane radiation patterns are presented at 4.9 GHz and 7.3 GHz frequencies, respectively. The comparison of the proposed antenna with the models in the literature survey is tabulated in Table 4.

4. CONCLUSION

An elliptical shape patch antenna operating for UWB in free space (3 to 10.7 GHz) and on a three-layered structure (2.2 to 10.8 GHz) is presented for on body communication. Inverted U-shaped slots are used to generate UWB, and CPW feed is used to produce impedance matching. As a result, the proposed antenna could potentially reduce the radiation impact on human body. The performance of antenna with respect to gain, radiation pattern, and SAR are presented. The SAR values of proposed antenna are within the standard limits.

ACKNOWLEDGMENT

This work was supported by the SERB, DST, New Delhi, India (Grant no: EEQ/2016/000754).

REFERENCES

1. Agneessens, S., P. van Torre, E. Tanghe, G. Verneeren, W. Joseph, and H. Rogier, "On-body wearable repeater as a data link relay for in-body wireless implants," *IEEE Antennas and Wireless Propagation Letters*, Vol. 11, 1714–1717, 2012.
2. Janapala, D. K., M. Nesasudha, and T. Mary Neebha, "SAR analysis of UWB antennas for wireless body area network applications," *Body Area Network Challenges and Solutions*, 105–129, Dec. 2018, doi: https://doi.org/10.1007/978-3-030-00865-9_6.
3. Alomainy, A., Y. Hao, C. Parini, and P. Hall, "Characterisation of printed UWB antennas for on-body communications," *IEE Wideband and Multi-band Antennas and Arrays*, 2005.
4. Adam, A. A., S. K. Abdul Rahim, K. G. Tan, and A. W. Reza, "Design of 3.1 to 12 GHz printed elliptical disc monopole antenna with half circular modified ground plane for UWB application," *Wireless Personal Communication*, Vol. 69, 535–549, 2013.
5. Kim, S. W. and D.-Y. Choi, "Implementation of rectangular slit-inserted ultra-wideband tapered slot antenna," *Springer Plus*, Vol. 5, 2016, doi: 10.1186/s40064-016-3033-4.
6. Kakhki, M. B. and P. Rezaei, "Reconfigurable microstrip slot antenna with DGS for UWB application," *EUCAP*, Vol. 9, 1517–1522, Sep. 2017.
7. Zhong, Y.-W., G.-M. Yang, and L.-R. Zheng, "Planar circular patch with elliptical slot antenna for ultrawideband communication application," *Microwave and Optical Technology Letters*, Vol. 57, No. 2, 325–328, 2015.
8. Huang, C. Y. and W. C. Hsia, "Planar elliptical antenna for ultrawideband communication," *Electronics Letters*, Vol. 41, No. 6, 296–297, 2005.
9. Catherwood, P. A., S. S. Bukhari, G. Watt, W. G. Whittow, and J. McLaughlin, "Body-centric wireless hospital patient monitoring network using body-contoured flexible antennas," *IET Microwaves, Antennas & Propagation*, Vol. 12, No. 2, 203–210, 2018.
10. Bhattacharyya, S., A. Bhattacharya, and I. Sarkar, "An ultra-wideband microstrip antenna with dual-band filtering for biomedical application," *Advancements of Medical Electronics*, 293–306, Jan. 2015.
11. Chi, Y.-J. and F.-C. Chen, "On body adhesive-bandage-like antenna for wireless medical telemetry services," *IEEE Transactions on Antennas and Propagation*, Vol. 62, No. 5, 2472–2480, May 2014.
12. See, T. S. P. and Z. N. Chen, "Experimental characterization of UWB antennas for on-body communications," *IEEE Transactions on Antennas and Propagation*, Vol. 57, No. 4, 866–874, Apr. 2009.

13. Cheng, S., P. Hallbjorner, and A. Rydberg, "Printed slot planar inverted cone antenna for ultrawideband applications," *IEEE Antennas and Wireless Propagation Letters*, Vol. 7, 18–21, 2008.
14. Lui, W. J., C. H. Cheng, and H. B. Zhu, "Compact frequency notched ultra-wideband fractal printed slot antenna," *IEEE Microwave and Wireless Components Letters*, Vol. 16, No. 4, 224–226, Apr. 2006.
15. Bharadwaj, R., C. Parini, S. K. Koul, and A. Alomainy, "Effect of limb movements on compact UWB wearable antenna radiation performance for healthcare monitoring," *Progress In Electronics Research C*, Vol. 91, 15–26, 2019.
16. Kumar, B. K., P. V. V. Kishore, and K. K. Naik, "Design of rectangular patch antenna with X-slots for wireless communications," *2018 Second International Conference on Inventive Communication and Computational Technologies (ICICCT)*, 1448–1451, 2018, doi: 10.1109/ICICCT.2018.8473111.
17. Alomainy, A., A. Sani, A. Rahman, J. G. Santas, and Y. Hao, "Transient characteristics of wearable antennas and radio propagation channels for ultrawideband body-centric wireless communications," *IEEE Transactions on Antennas and Propagation*, Vol. 57, No. 4, 875–884, Apr. 2009.
18. Raad, H. K., H. M. Al-Rizzo, A. Abbosh, and A. I. Hammoodi, "A compact dual band polyimide based antenna for wearable and flexible telemedicine devices," *Progress In Electromagnetics Research C*, Vol. 63, 153–161, 2016.
19. Kumar Naik, K., S. Chaithanya Satya Teja, B. V. S. Sailaja, and P. A. Sri, "Design of flexible parasitic element patch antenna for biomedical application," *Progress In Electromagnetics Research M*, Vol. 94, 143–153, 2020.
20. Ketavath, K. N., D. Gopi, and S. S. Rani, "In-vitro test of miniaturized CPW-fed implantable conformal patch antenna at ISM band for biomedical applications," *IEEE Access*, Vol. 7, 43547–43554, Mar. 2019.